

Ionic Encapsulation of a Methanol Carbonylation Catalyst in a Microporous Metal-Organic Framework

Electronic Supplementary Information (ESI)

Samuel A. Ivko,^{a,c} Tom Bailey,^{b,c} Lee Brammer^c and Anthony Haynes^{*c}

^a School of Chemistry, University of Birmingham, Birmingham B15 2TT, UK.

^b School of Chemical and Process Engineering, University of Leeds, Leeds LS2 9JT, UK.

^c Department of Chemistry, University of Sheffield, Sheffield S3 7HF, UK. E-mail: a.haynes@sheffield.ac.uk

Contents

S1.	General	2
S1.1.	Materials	2
S1.2.	Instrumentation and Analytical methods	2
S2.	Synthetic and catalytic reactions.....	5
S2.1.	Synthesis of 2-(imidazol-1-yl)dicarboxylic acid (H ₂ BDC-Im).....	5
S2.2.	Synthesis of 1-(2,5-dicarboxyphenyl)-3-methyl-1 <i>H</i> -imidazol-3-ium iodide ([H ₂ BDC-Im-Me][I])	5
S2.3.	Synthesis of [Zr ₆ O ₄ (OH) ₄ (BDC) ₆] (UiO-66).....	6
S2.4.	Synthesis of [Zr ₆ O ₄ (OH) ₄ (BDC-Im) ₆]	7
S2.5.	Synthesis of [Zr ₆ O ₄ (OH) ₄ (BDC-Im) _{0.9} (BDC-Im-Me) _{5.1}][I] _{5.1}	8
S2.6.	Synthesis of [Zr ₆ O ₄ (OH) ₄ (BDC) _{4.8} (BDC-Im) _{1.1} (OAc) _{0.1}] (1)	11
S2.7.	Synthesis of [Zr ₆ O ₄ (OH) ₄ (BDC) _{4.8} (BDC-Im-Me) _{1.1} (OAc) _{0.1}][I] _{1.1} (2)	13
S2.8.	Synthesis of [Zr ₆ O ₄ (OH) ₄ (BDC) _{4.8} (BDC-Im-Me) _{1.1} (OAc) _{0.1}][Rh(CO) ₂ I ₂] _{1.1} (3)...15	
S2.9.	Synthesis of [Zr ₆ O ₄ (OH) ₄ (BDC) _{4.8} (BDC-Im-Rh(CO) ₂ I) _{1.1} (OAc) _{0.1}]	16
S2.10.	Reaction of 3 with MeI and CO	17
S2.11.	Catalytic carbonylation of MeOH with 3	17
S3.	Pawley fitting parameters	20
S4.	References	21

S1.General

S1.1. Materials

Dry CHCl_3 and *n*-hexane were obtained from a Grubbs solvent purification system in which the solvents were degassed with N_2 prior to being passed through activated alumina and a supported copper catalyst to remove protic contaminants and trace oxygen respectively.¹ These solvents were stored under N_2 . Solvents were used within 24 h of collection from the dry solvent system. Other solvents were purchased from either Fisher Scientific or Sigma Aldrich (HPLC grade unless otherwise stated) and were used without further purification. Standard Schlenk techniques and glassware were used for preparative reactions. $[\text{Rh}(\text{CO})_2\text{I}]_2$ was prepared according to a literature procedure.² Carbon monoxide (99.9% CP grade) was supplied by BOC. All other reagents were purchased from either Fisher Scientific or Sigma Aldrich and used without further purification.

S1.2. Instrumentation and Analytical methods

Infra-red spectra of solid samples were collected using a Perkin-Elmer 100 FTIR spectrometer either with an ATR accessory or as KBr disks, prepared by grinding the sample with a 20-fold excess of pure KBr dried overnight in a vacuum oven at 80 °C. The samples were pelletized at high pressure (10 tons) and analysed as a thin transparent disk.

Solution-phase ^1H and $^{13}\text{C}\{^1\text{H}\}$ NMR spectra were collected using a Bruker AC400 spectrometer fitted with an automatic sample changer using the solvent as the internal standard. MOF samples were digested for analysis by solution phase NMR spectroscopy using one of the following methods:

To digest in a mixture of $\text{NaOD}/\text{D}_2\text{O}$, the sample was added to a capped sample vial to which D_2O (1 cm^3) and NaOD (40% w/w in D_2O , 0.05 cm^3) were added. The mixture was sonicated for 10 minutes and then filtered through cotton wool before analysis.

To digest in a mixture of D_3PO_4 with D_2O or $(\text{CD}_3)_2\text{SO}$, the sample was added to a capped sample vial to which D_2O or $(\text{CD}_3)_2\text{SO}$ (1 cm^3) and D_3PO_4 (85% w/w in D_2O , 0.25 cm^3) were added. The mixture was stirred overnight and then filtered through cotton wool before analysis.

For solid-state NMR, the sample was packed into a 4 mm zirconia rotor and transferred to a Bruker Avance III HD spectrometer. 1D ^1H - ^{13}C cross-polarisation magic angle spinning

(CP/MAS) NMR measured were obtained at 125.76 MHz (500.13 MHz ^1H) at a MAS rate of 10.0 kHz. The ^1H $\pi/2$ pulse was 3.4 μs , and two-pulse phase modulation (TPPM) decoupling was used during the acquisition. The Hartmann-Hahn condition was set using hexamethylbenzene. The spectra were measured using a contact time of 2.0 ms. The relaxation delay, D_1 , for each sample was individually determined from the proton T_1 measurement ($D_1 = 5 \times T_1$). Scans were collected until sufficient signal to noise ratio was observed, typically greater than 1094 scans. The values of the chemical shifts are referenced to that of TMS.

For powder X-ray diffraction pattern collection, samples were dried under high vacuum before being ground into a fine powder using a pestle and mortar. The microcrystalline sample was then analysed using a Bruker D8 Advance X-ray powder diffractometer equipped with a LynxEye Detector, a Cu K_α sealed tube source ($\lambda = 1.5406 \text{ \AA}$) and a variable motorised slit. Patterns were recorded in Debye-Scherrer geometry (in a capillary stage with samples loaded in 0.7 mm borosilicate capillaries and rotated at 30 rpm). Intensity data were collected between 5° to 70° 2θ at 0.02° increments and step time of 1 s (other than the recovered solid after the catalysis experiment which had a step time of 0.1 s). Data were collected under ambient conditions. Indexing and Pawley refinements³ were carried out using TOPAS Academic version 4.1.⁴⁻⁶ Details of all Pawley fits can be found in Section S3.

Nitrogen gas sorption isotherms were collected at 77 K using approximately 100 mg of sample on an ASAP 2020 micromeritics volumetric adsorption analyser. Prior to analysis all samples except those with encapsulated *cis*- $[\text{Rh}(\text{CO})_2\text{I}_2]$ were degassed for at least 16 h at 120°C under a vacuum of at least 10^{-5} bar. Samples containing rhodium were degassed under the same vacuum level but without heating due to issues relating to the stability of the complex. BET surface areas were calculated over a relative pressure range (p/p_0) of between 0.01 – 0.15. Pore size distributions and pore volumes were calculated from the adsorption isotherms and modelled using the nonlocal density functional theory model (NL-DFT) for N_2 on carbon slit pores found within the micromeritics ASAP software (Table S1).

Table S1 Surface areas and pore volumes of MOF samples **1-3** and UiO-66.

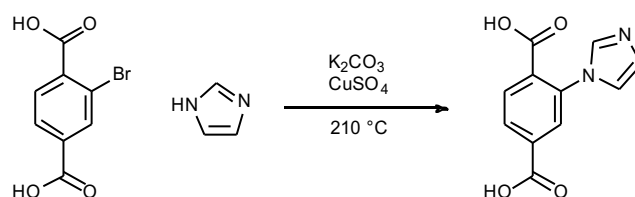
Sample	SA _{BET} ^a / m ² g ⁻¹	V _{tot} ^b / cm ³ g ⁻¹	V _{0.1} ^c / cm ³ g ⁻¹	(V _{0.1} /V _{tot})
UiO-66	1238	0.71	0.53	0.75
1	1139	0.55	0.49	0.89
2	1031	0.50	0.43	0.86
3	477	0.24	0.20	0.83

^a Calculated over the pressure range 0.01-0.15 p/p_0 . ^b Calculated at 0.99 p/p_0 . ^c Calculated at 0.1 p/p_0 .

Carbon, hydrogen and nitrogen elemental analysis was performed by the University of Sheffield Department of Chemistry Microanalysis Service by burning a small amount of sample in a stream of pure oxygen. The sample was placed in a tin capsule and introduced into the combustion tube of the Elementar Vario MICRO Cube CHN/S analyser via a stream of helium. Combustion products were analysed by first passing the sample through a copper tube to remove excess oxygen and reduce any NO_x to N₂. Gases were separated using a Thermal Programmed Desorption column and detected using a Thermal Conductivity Detector. Iodide analysis was performed using the Schöninger flask combustion method in which an amount of sample is combusted in an oxygen-enriched environment, the resultant gases are absorbed, and a titration is conducted to determine the iodide concentration. Rhodium analysis was performed by inductively coupled plasma - optical emission spectroscopy (ICP-OES) using a Spectro Ciros Vision instrument.

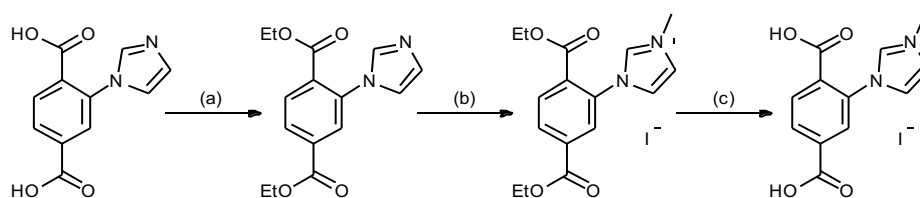
S2. Synthetic and catalytic reactions

S2.1. Synthesis of 2-(imidazol-1-yl)dicarboxylic acid (H₂BDC-Im)



The linker was synthesised according to a modified procedure from the literature.⁷ Imidazole (8.500 g, 125 mmol), 2-bromoterephthalic acid (6.125 g, 25 mmol), K₂CO₃ (9.674 g, 70 mmol) and CuSO₄ (0.250 g, 1 mmol) were ground together and added to a 125 cm³ solvothermal vessel which had been flushed with Ar. The mixture was sealed and incubated at 210 °C for 10 h before cooling to room temperature. The crude solid product was dissolved in H₂O (300 cm³) and filtered. The pH of the filtrate was adjusted to between 2 and 3 with 6 M HCl. The grey precipitate was isolated by filtration and recrystallised from 6 M HCl. The product was heated at 80 °C under vacuum for 16 h to yield 2-(imidazol-1-yl)benzene-1,4-dicarboxylic acid (3.182 g, 47%) as light brown crystals, (Found: C, 49.0; H, 3.4; N, 10.5; Cl, 13.4. C₁₁H₉N₂O₄Cl expected: C, 49.2; H, 3.4; N, 10.4; Cl, 13.2%); δ_{H} (400 MHz; D₂O and D₃PO₄) 6.81 (s, 1 H), 6.84 (s, 1 H), 7.35 (s, 1 H), 7.45 (br. m, 2 H), 8.13 (s, 1 H); δ_{C} (400 MHz; D₂O and D₃PO₄) 118.77, 123.00, 128.31, 129.84, 131.33, 131.82, 133.37, 134.19, 135.11, 165.83, 166.96; m/z 233 (100%, M⁺).

S2.2. Synthesis of 1-(2,5-dicarboxyphenyl)-3-methyl-1*H*-imidazol-3-ium iodide ([H₂BDC-Im-Me][I])

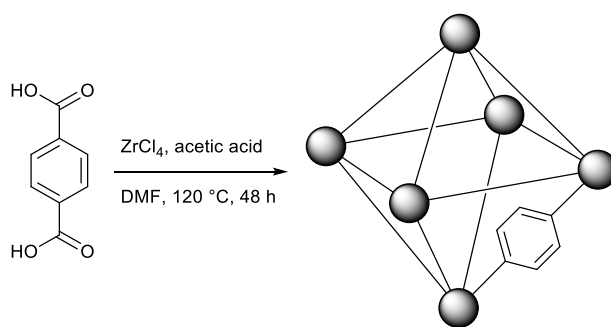


(a) EtOH/DMF, SOCl₂ dropwise, reflux 72 h, (b) MeI/MeCN, reflux 24 h, (c) 6 M HCl reflux 16 h.

This reaction was performed according to a modified procedure from the literature.⁸ 2-(imidazol-1-yl)benzene-1,4-dicarboxylic acid (5.166 g, 19.2 mmol) was dissolved in EtOH (64 cm³) and DMF (3 drops). SOCl₂ (7 cm³, 96.4 mmol) was added dropwise. The mixture was refluxed at 80 °C for 48 h, and then the solvent was removed under reduced pressure. The crude

product was dissolved in H₂O (40 cm³) and the pH was adjusted to above 9 with 2M aq. KOH. The solution was extracted with EtOAc (4 × 70 cm³) and the organic layers were combined and dried over MgSO₄. The solvent was removed under reduced pressure. The white solid product was dissolved in MeCN (52 cm³) and MeI (13 cm³, 208.8 mmol) and refluxed at 80 °C for 72 h. Solvent was removed under reduced pressure and the solid product was dissolved in 6 M aq. HCl (32 cm³) and refluxed for 16 h. The mixture was allowed to cool, at which point the product precipitated. This was collected by filtration and dried in a vacuum oven for 16 h to yield 1-(2,5-dicarboxyphenyl)-3-methyl-1*H*-imidazol-3-ium iodide (2.171 g, 30%) as a yellow powder, δ_H (400 MHz; D₂O and D₃PO₄) 3.20 (s, 3 H), 6.79 (s, 1 H), 6.83 (s, 1 H), 7.35 (s, 1 H), 7.46 (br. m, 2 H), 8.12 (s, 1 H); δ_C (400 MHz; D₂O and D₃PO₄) 35.45, 122.74, 123.44, 128.31, 129.85, 131.38, 131.86, 133.31, 134.24, 136.36, 165.85, 167.00; m/z 247 (100%, M⁺).

S2.3. Synthesis of [Zr₆O₄(OH)₄(BDC)₆] (UiO-66)



Unsubstituted UiO-66 was synthesised using a literature procedure.⁷ Benzene-1,4-dicarboxylic acid (483 mg, 2.9 mmol) and ZrCl₄ (683 mg, 2.9 mmol) were dissolved in dry DMF (70 cm³). To this was added acetic acid (17 cm³). This mixture was left to stir for 1 h before being added into a 125 cm³ Teflon-lined stainless steel autoclave. This was incubated at 120 °C for 48 h, with a ramping rate of 1 °C min⁻¹ and a cooling rate of 0.1 °C min⁻¹. Once cooled to room temperature, the product was collected via centrifugation and washed with DMF (2 × 70 cm³), followed by leaving to stand in MeOH for 72 h, exchanging for fresh solvent every 24 h. Finally, the product was dried under high vacuum for 16 h, to give [Zr₆O₄(OH)₄(BDC)₆] (0.594 g, 74% based on zirconium) as a white powder. The powder pattern (Figure S1) was fitted using TOPAS Academic version 4.1 as an *Fm* $\bar{3}$ *m* space group where *a* = 20.8054(5) Å (Section S3).

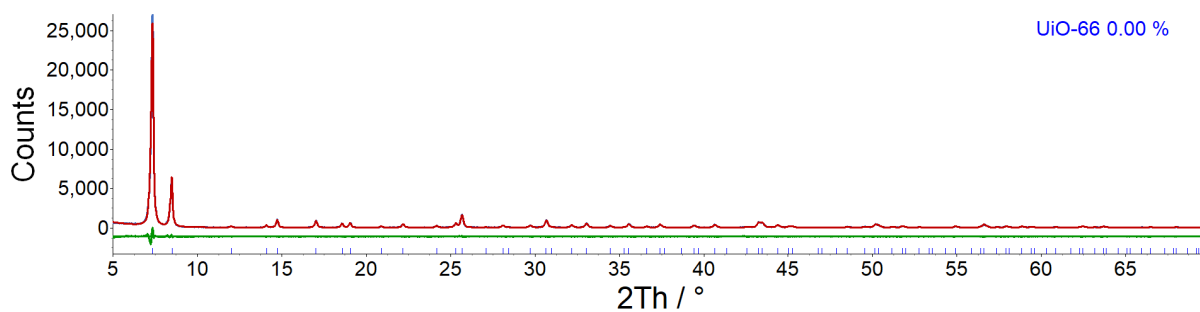
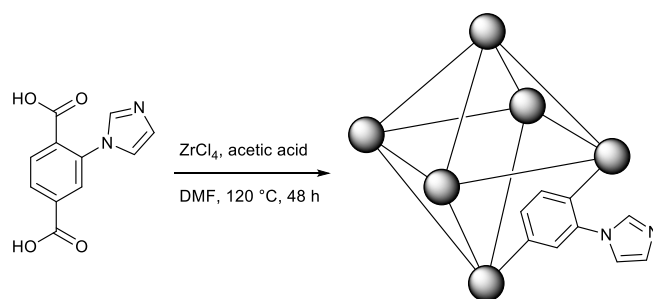


Figure S1 Pawley fit of UiO-66 showing the observed pattern (blue), the fit (red), and the difference (green).

S2.4. Synthesis of $[\text{Zr}_6\text{O}_4(\text{OH})_4(\text{BDC-Im})_6]$



The MOF was synthesised according to a modification of a literature procedure.⁷ 2-(imidazol-1-yl)benzene-1,4-dicarboxylic acid (2.497 g, 8.7 mmol) and ZrCl_4 (2.031 g, 8.7 mmol) were dissolved in dry DMF (208 cm^3). To this was added acetic acid (50 cm^3). This mixture was left to stir for 1 h before being separated into 3 equal portions and added into $3 \times 125 \text{ cm}^3$ Teflon-lined stainless steel autoclaves. These were incubated at 120 °C for 48 h, with a ramping rate of 1 °C min^{-1} and a cooling rate of 0.1 °C min^{-1} . Once cooled to room temperature, the products were combined and collected via centrifugation and washed with DMF ($2 \times 200 \text{ cm}^3$), followed by leaving to stand in MeOH for 72 h, exchanging for fresh solvent every 24 h. Finally, the product was dried under high vacuum for 16 h, to give $[\text{Zr}_6\text{O}_4(\text{OH})_4(\text{BDC-Im})_6]$ (2.193 g, 66% based on zirconium) as a white powder, (Found: C, 31.5; H, 2.9; N, 7.2; Cl, 3.7. Expected: C, 37.2; H, 2.0; N, 7.9; Cl, 3.3% assuming one-third of imidazolyl groups in hydrochloride form to account for Cl content); δ_{H} (400 MHz; $(\text{CD}_3)_2\text{SO}$ and D_3PO_4) 6.82 (s, 1 H), 6.86 (s, 1 H), 7.37 (s, 1 H), 7.47 (br. m, 2 H), 8.14 (s, 1 H); δ_{C} (400 MHz; $(\text{CD}_3)_2\text{SO}$ and D_3PO_4) 118.78, 123.02, 128.33, 129.87, 131.35, 131.84, 133.39, 134.21, 135.13, 165.86, 169.99. The powder pattern (Figure S2) was fitted using TOPAS Academic version 4.1 as an $Fm\bar{3}m$ space group where $a = 20.7881(3) \text{ \AA}$ (Section S3).

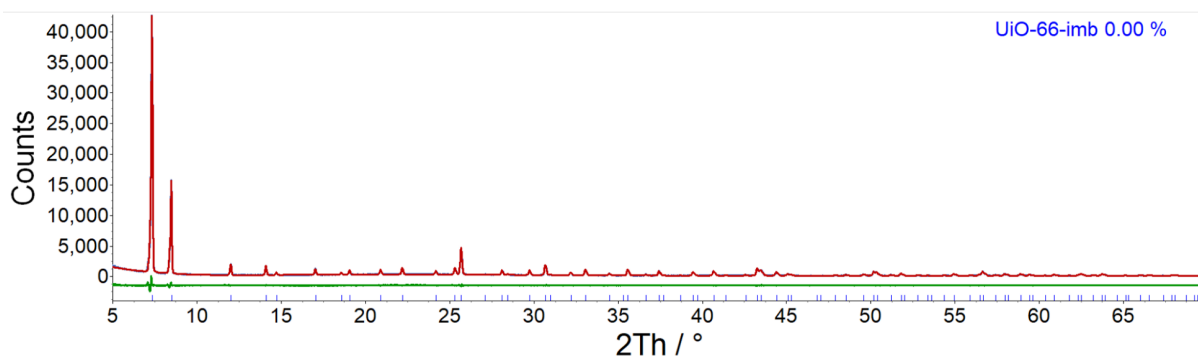


Figure S2 Pawley fit of $[\text{Zr}_6\text{O}_4(\text{OH})_4(\text{BDC-Im})_6]$ showing the observed pattern (blue), the fit (red), and the difference (green). $5 \leq 2\theta \leq 70^\circ$; $d_{\min} 1.34 \text{ \AA}$.

The solid-state CP-MAS $^{13}\text{C}\{^1\text{H}\}$ NMR spectrum of $[\text{Zr}_6\text{O}_4(\text{OH})_4(\text{BDC-Im})_6]$ contains broad signals in the expected regions based on the solution-phase $^{13}\text{C}\{^1\text{H}\}$ NMR spectrum of $\text{H}_2\text{BDC-Im}$ in $(\text{CD}_3)_2\text{SO}$, as well as weak resonances at 20.4 ppm and 29.9 ppm thought to be due to residual acetic acid and silicone grease respectively (Figure S3).

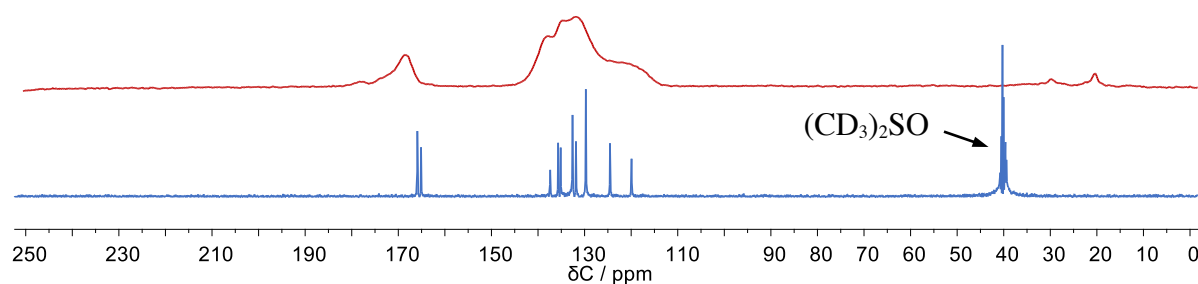
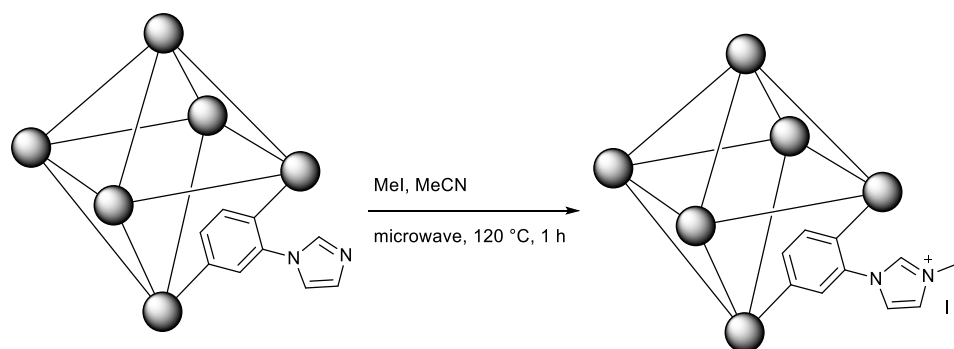


Figure S3 Solution-phase $^{13}\text{C}\{^1\text{H}\}$ NMR spectrum of $\text{H}_2\text{BDC-Im}$ (blue, in $(\text{CD}_3)_2\text{SO}$) and solid-state CP-MAS $^{13}\text{C}\{^1\text{H}\}$ NMR spectrum of $[\text{Zr}_6\text{O}_4(\text{OH})_4(\text{BDC-Im})_6]$ (red).

S2.5. Synthesis of $[\text{Zr}_6\text{O}_4(\text{OH})_4(\text{BDC-Im})_{0.9}(\text{BDC-Im-Me})_{5.1}][\text{I}]_{5.1}$



The cationic MOF was synthesised via postsynthetic modification of $[\text{Zr}_6\text{O}_4(\text{OH})_4(\text{BDC-Im})_6]$. $[\text{Zr}_6\text{O}_4(\text{OH})_4(\text{BDC-Im})_6]$ (0.400 g, ~ 0.23 mmol) was added to a 10 cm^3 microwave tube with

dry MeCN (3 cm³) and MeI (1 cm³). The tube was heated to 120 °C in a microwave reactor (Discover Explorer microwave synthesiser) for 1 h with stirring, reaching a pressure of 6 bar, before drying under vacuum overnight to give [Zr₆O₄(OH)₄(BDC-Im)_{0.9}(BDC-Im-Me)_{5.1}][I]_{5.1} (0.369 g) as a yellow powder, (Found: C, 28.5; H, 2.6; N, 1.2. Expected: C, 29.7; H, 2.0; N, 5.8%); δ_H (400 MHz; D₂O and D₃PO₄) 3.22 (s, 2.6 H), 6.79 (m, 2 H), 7.40 (m, 3 H), 8.09 (m, 1 H); δ_C (400 MHz; D₂O and D₃PO₄) 35.45, 122.74, 123.47, 128.34, 129.90, 131.41, 131.88, 133.33, 134.27, 136.39, 165.91, 167.07; m/z (EI, (CD₃)₂SO and D₃PO₄) 247 (100%, M⁺), 233 (6%, M⁺ - CH₃). The powder pattern (Figure S4) was fitted using TOPAS Academic version 4.1 as an *Fm* $\bar{3}$ *m* space group where *a* = 20.813(1) Å (Section S3).

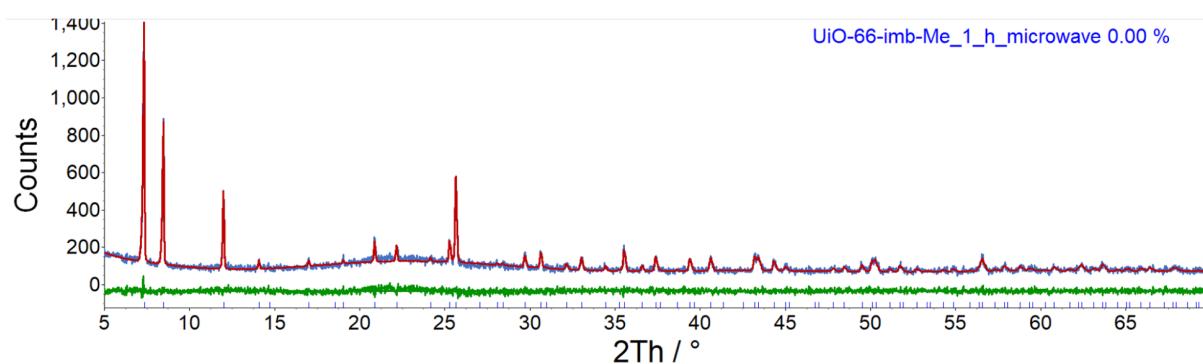


Figure S4 Pawley fit of [Zr₆O₄(OH)₄(BDC-Im)_{0.9}(BDC-Im-Me)_{5.1}][I]_{5.1} showing the observed pattern (blue), the fit (red), and the difference (green). 5 ≤ 2θ ≤ 70 °; *d*_{min} 1.34 Å.

The product was digested in D₃PO₄ / D₂O for analysis by ¹H NMR spectroscopy to determine the extent of quaternisation. In the solution-phase ¹H NMR spectrum of the digested product, the aromatic resonances due to the neutral and quaternised linkers overlap one another (Figure S5). Therefore, in order to calculate extent of quaternisation, the intensity of one of the combined aromatic resonances (at 8.09 ppm) is compared with the *N*-methyl resonance (at 3.14 ppm). The relative integrals of these resonances are 1.00 and 2.56 respectively. If the reaction had reached 100% conversion, the *N*-methyl resonance would have an integration value of 3.00. The reaction is therefore calculated to have reached 85% conversion of imidazole to *N*-methylimidazolium groups, giving a formula of [Zr₆O₄(OH)₄(BDC-Im)_{0.9}(BDC-Im-Me)_{5.1}][I]_{5.1}.

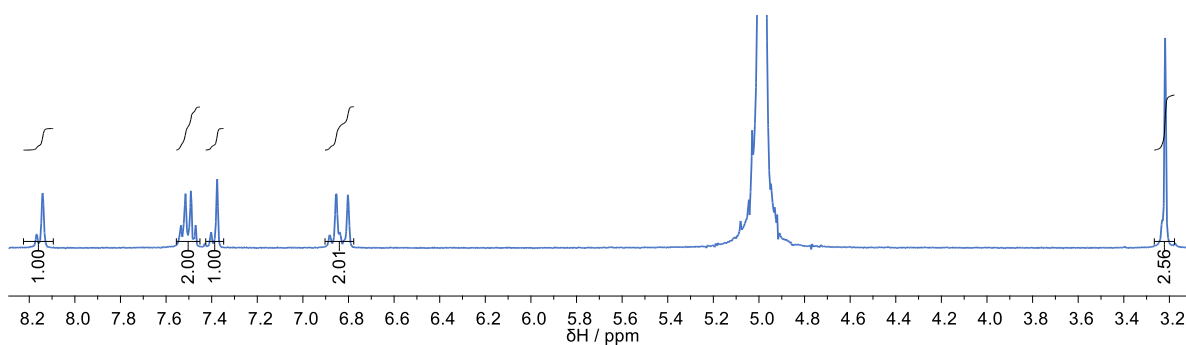


Figure S5 Solution-phase ^1H NMR spectrum of $[\text{Zr}_6\text{O}_4(\text{OH})_4(\text{BDC-Im})_{0.9}(\text{BDC-Im-Me})_{5.1}][\text{I}]_{5.1}$ digested in $\text{D}_3\text{PO}_4 / \text{D}_2\text{O}$.

Solid-state CP-MAS $^{13}\text{C}\{^1\text{H}\}$ NMR spectroscopy confirmed the successful quaternisation of imidazole groups in the MOF, with an extra resonance at 37 ppm consistent with that for the *N*-methyl carbon atom in the solution-phase $^{13}\text{C}\{^1\text{H}\}$ NMR spectrum of $[\text{H}_2\text{BDC-Im-Me}][\text{I}]$ in $(\text{CD}_3)_2\text{SO}$ (Figure S6).

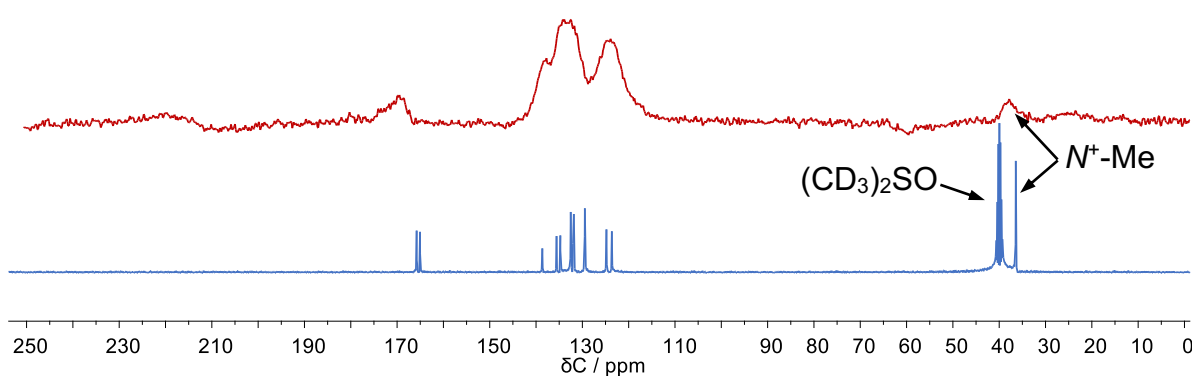
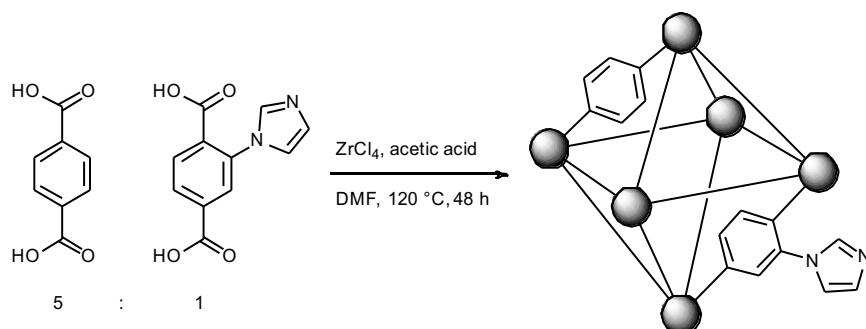


Figure S6 Solution-phase $^{13}\text{C}\{^1\text{H}\}$ NMR spectrum of $[\text{H}_2\text{BDC-Im-Me}][\text{I}]$ (blue, in $(\text{CD}_3)_2\text{SO}$) and solid-state CP-MAS $^{13}\text{C}\{^1\text{H}\}$ NMR spectrum of $[\text{Zr}_6\text{O}_4(\text{OH})_4(\text{BDC-Im})_{0.9}(\text{BDC-Im-Me})_{5.1}][\text{I}]_{5.1}$ (red).

S2.6. Synthesis of $[\text{Zr}_6\text{O}_4(\text{OH})_4(\text{BDC})_{4.8}(\text{BDC-Im})_{1.1}(\text{OAc})_{0.1}]$ (**1**)



ZrCl_4 (2.055 g, 8.8 mmol), benzene-1,4-dicarboxylic acid (1.205 g, 7.3 mmol), 2-(imidazol-1-yl)benzene-1,4-dicarboxylic acid (0.389 g, 1.5 mmol) were dissolved in a mixture of acetic acid (50 cm³) and dry DMF (208 cm³). The solution was divided into three equal portions which were added to 3 × 125 cm³ Teflon-lined stainless steel autoclaves and incubated at 120 °C for 48 h, with a ramping rate of 1 °C min⁻¹ and a cooling rate of 0.1 °C min⁻¹. Once cooled to room temperature, the products were combined and collected via centrifugation and washed with DMF (2 × 200 cm³), and soaked in MeOH for 72 h, exchanging for fresh solvent every 24 h. Finally, the product was dried under high vacuum for 16 h, to give mixed-linker $[\text{Zr}_6\text{O}_4(\text{OH})_4(\text{BDC})_{4.8}(\text{BDC-Im})_{1.1}(\text{OAc})_{0.1}]$ (**1**) (2.477 g, 89% based on zirconium) as a white powder, (Found: C, 32.6; H, 2.6; N, 1.5. Expected: C, 35.3; H, 1.8; N, 1.8%); δ_{H} (400 MHz; D₂O and NaOD) 2.12 (s, 3 H), 7.03 (s, 1 H), 7.22 (s, 1 H), 7.45 (d, $J = 8.0$ Hz, 1 H), 7.71 (m, 2 H), 7.74 (s, 16 H), 7.80 (dd, $J = 8.0, 1.5$ Hz, 1 H). The powder pattern (Figure S7) was fitted using TOPAS Academic version 4.1 as an $Fm\bar{3}m$ space group where $a = 20.739(2)$ Å (Section S3). An IR spectrum of **1** is shown in Figure S8.

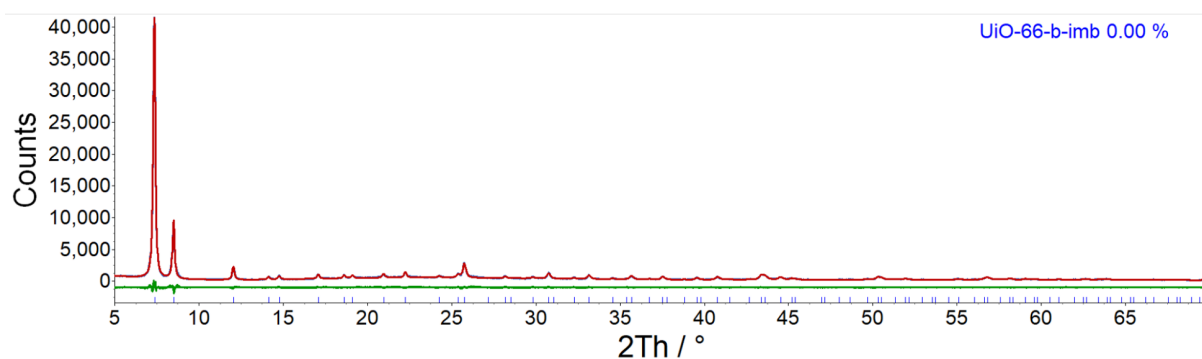


Figure S7 Pawley fit of **1** showing the observed pattern (blue), the fit (red), and the difference (green). $5 \leq 2\theta \leq 70$ °; $d_{\text{min}} 1.34$ Å.

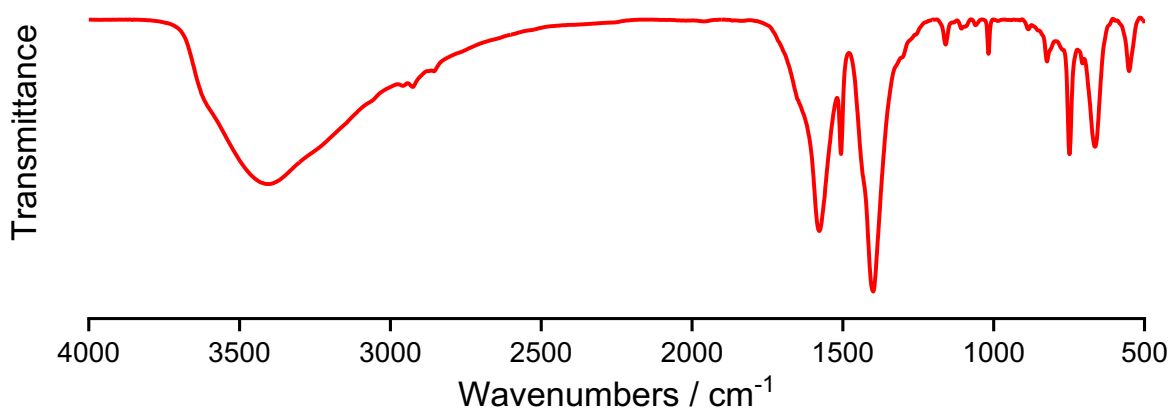


Figure S8 IR spectrum (KBr disc) of **1**.

In order to determine the linker ratios in **1**, the sample was digested in a solution of NaOD in D₂O and a solution-phase ¹H NMR spectrum was recorded (Figure S9). The linker BDC displays one resonance at 7.80 ppm in this solvent mixture (corresponding to four aromatic protons), whereas BDC-Im displays resonances at 7.09, 7.28, 7.52, 7.77 and 7.86 ppm (all corresponding to one aromatic proton, apart from the resonance at 7.86 ppm which corresponds to two). The resonance for BDC overlaps with the resonances at 7.77 and 7.86 ppm for BDC-Im in the spectrum of the digested product. These combined resonances give a relative intensity 20.10 times larger than the resonance at 7.09 ppm for BDC-Im. This intensity includes contribution of three protons in BDC-Im from the resonances at 7.77 and 7.86 ppm, meaning that the relative intensity due to BDC is actually 17.10. Acetic acid (AcOH) is also detectable in the spectrum (2.12 ppm) with a relative intensity of 0.30. This gives a final ratio for BDC : BDC-Im : OAc of 4.3:1:0.1, giving the final formula of the MOF as [Zr₆O₄(OH)₄(BDC)_{4.8}(BDC-Im)_{1.1}(OAc)_{0.1}].

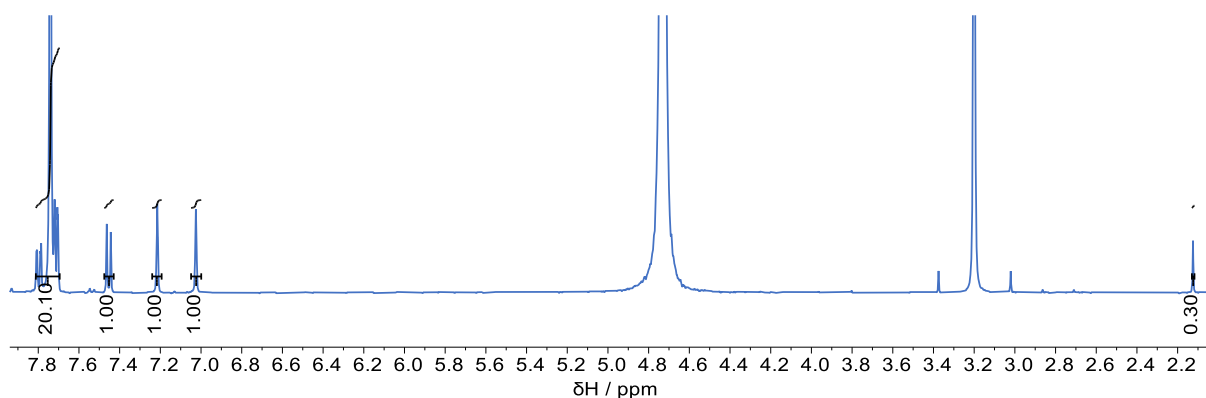
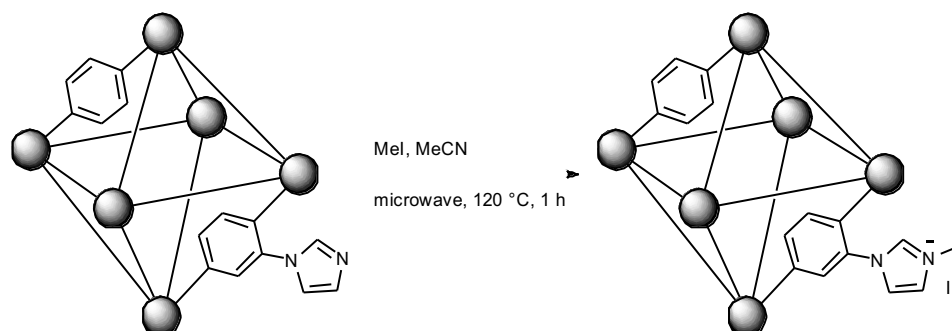


Figure S9 ¹H NMR spectrum of **1** digested in NaOD / D₂O.

S2.7. Synthesis of $[\text{Zr}_6\text{O}_4(\text{OH})_4(\text{BDC})_{4.8}(\text{BDC-Im-Me})_{1.1}(\text{OAc})_{0.1}][\text{I}]_{1.1}$ (**2**)



A sample of **1** (200 mg) was added to a microwave tube with dry MeCN (3 cm³) and MeI (1 cm³). This mixture was heated in the microwave reactor to 120 °C for 1 h with stirring, reaching a pressure of *ca.* 6 bar. The product was collected by centrifugation and washed with MeOH (2 × 20 cm³) before drying under high vacuum for 16 h to give the product (**2**) (186 mg) as an off-white powder, (Found: C, 28.5; H, 2.6; N, 1.2. Expected for $[\text{Zr}_6\text{O}_4(\text{OH})_4(\text{BDC})_{4.8}(\text{BDC-Im-Me})_{1.1}(\text{OAc})_{0.1}][\text{I}]_{1.1}$: C, 33.1; H, 1.8; N, 1.6%); δ_{H} (400 MHz; (CD₃)₂SO and D₃PO₄) 3.84 (s, 2.9 H), 7.52 (s, 1 H), 7.60 (s, 1 H), 7.96 (s, 16 H), 8.00 (s, 1 H), 8.16 (m, 2 H), 8.97 (s, 1 H). The powder pattern (Figure S10) was fitted using TOPAS Academic version 4.1 as an $Fm\bar{3}m$ space group where $a = 20.750(1)$ Å (Section S3). An IR spectrum of **2** is shown in Figure S11.

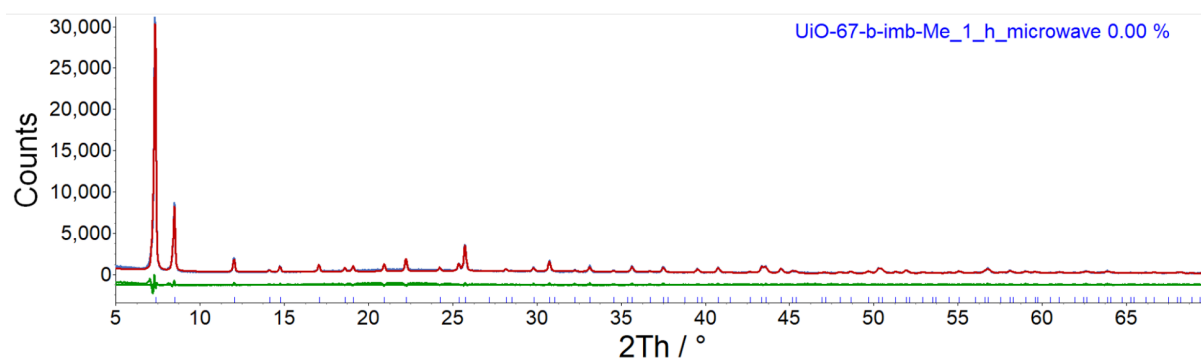


Figure S10 Pawley fit of **2** showing the observed pattern (blue), the fit (red), and the difference (green). $5 \leq 2\theta \leq 70$ °; $d_{\text{min}} 1.34$ Å.

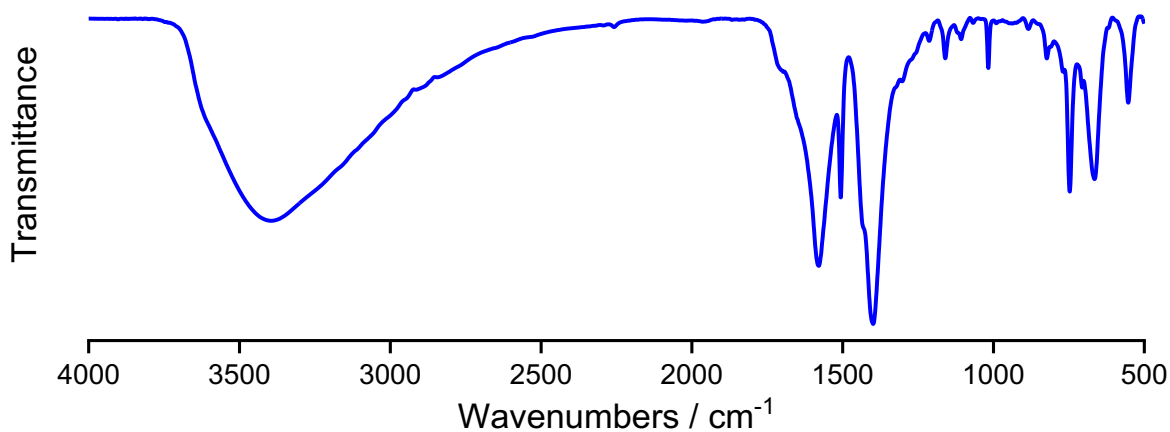


Figure S11 IR spectrum (KBr disc) of **2**.

2 was digested in D_3PO_4 / D_2O and its 1H NMR spectrum was recorded to determine the extent of quaternisation of imidazole sites (Figure S12). The resonances due to imidazole and *N*-methylimidazolium overlap in the spectrum, and so the extent of quaternisation is determined by comparing the relative intensities of one of these combined resonances (at 8.11 ppm) with the *N*-methyl resonance (at 3.19 ppm). The resonance at 3.19 ppm had an intensity 2.95 times larger than the resonance at 8.11 ppm, indicating conversion of 98% of imidazole sites to *N*-methylimidazolium, giving a formula of $[Zr_6O_4(OH)_4(BDC)_{4.8}(BDC-Im-Me)_{1.1}(OAc)_{0.1}][I]_{1.1}$.

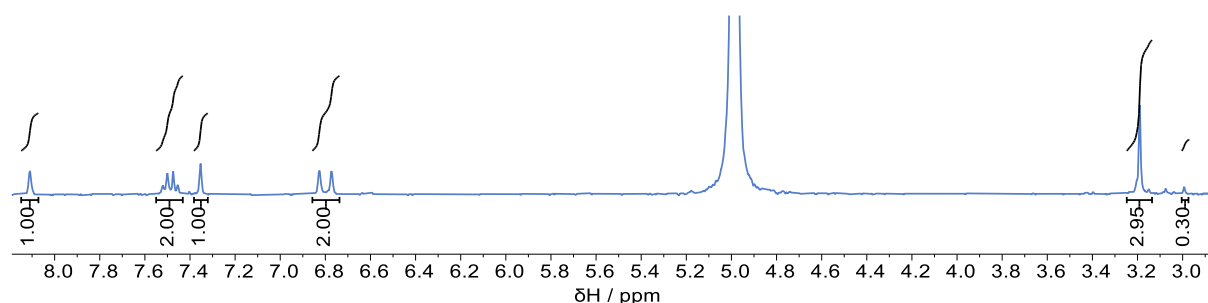
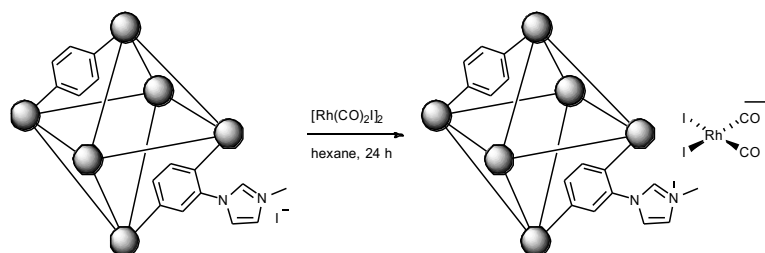


Figure S12 Solution-phase 1H NMR spectrum of **2** digested in D_3PO_4 / D_2O .

S2.8. Synthesis of $[\text{Zr}_6\text{O}_4(\text{OH})_4(\text{BDC})_{4.8}(\text{BDC-Im-Me})_{1.1}(\text{OAc})_{0.1}][\text{Rh}(\text{CO})_2\text{I}_2]_{1.1}$ (**3**)



Dry *n*-hexane (20 cm³) was added to a mixture of **2** (150 mg) and $[\text{Rh}(\text{CO})_2\text{I}]_2$ (27 mg, 0.04 mmol) under CO gas. The mixture was stirred at RT for 16 h. Solids were collected *via* centrifugation and washed with dry *n*-hexane (2 × 20 cm³) before drying under high vacuum for 1 h to give the product (**3**) as a brown powder (145 mg), $\nu(\text{CO}) / \text{cm}^{-1}$ (KBr disc) 2060 (s), 1986 (s). The product was stored at *ca.* 5 °C under CO. The powder pattern (Figure S13) was fitted using TOPAS Academic version 4.1 as an $Fm\bar{3}m$ space group where $a = 20.760(1)$ Å (Section S3). An IR spectrum of **3** is shown in Figure S14. Figure S15 shows IR spectra of products **1**, **2** and **3** for comparison, highlighting the $\nu(\text{CO})$ region.

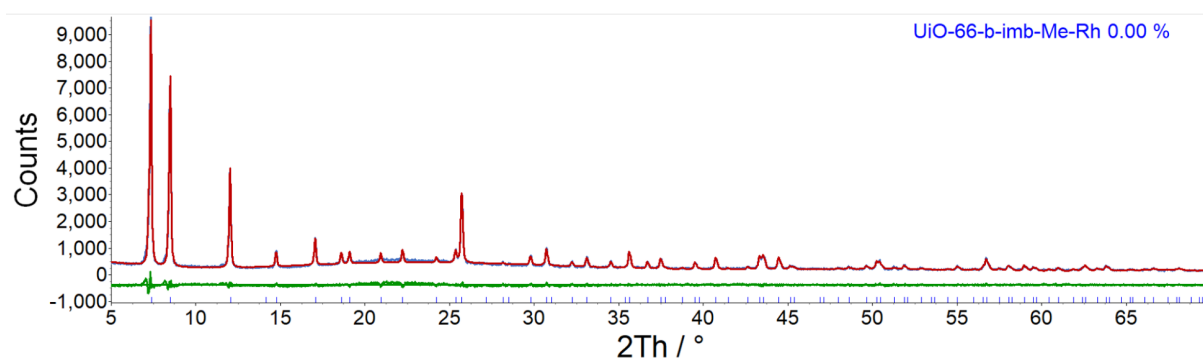


Figure S13 Pawley fit of **3** showing the observed pattern (blue), the fit (red), and the difference (green). $5 \leq 2\theta \leq 70$ °; $d_{\text{min}} 1.34$ Å.

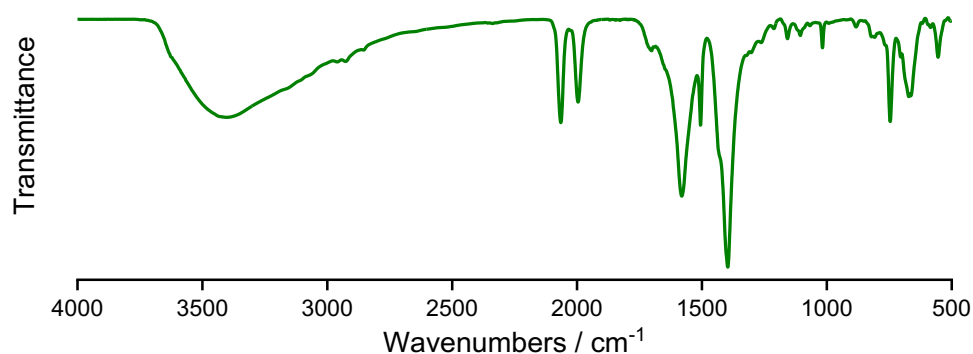


Figure S14 IR spectrum (KBr disc) of **3**.

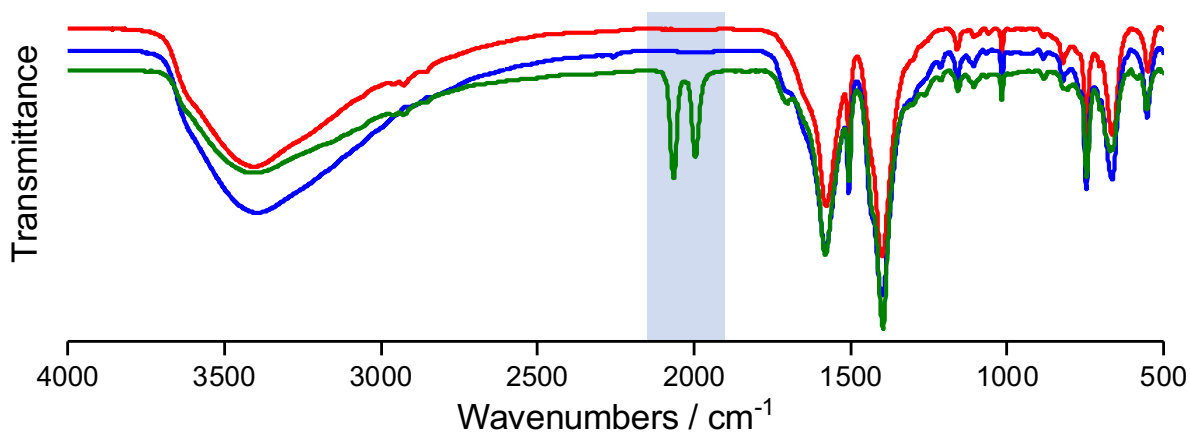
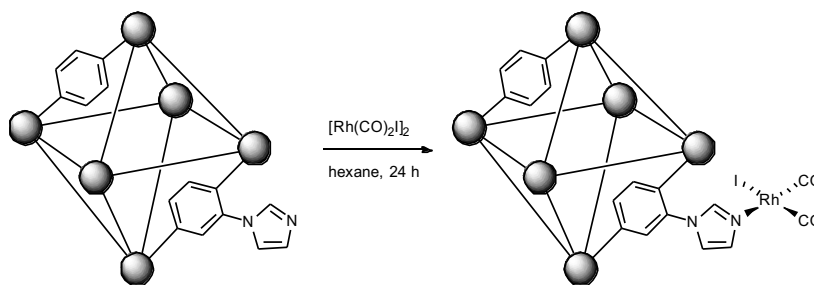


Figure S15 IR spectra (KBr disc) of samples 1-3 (terminal $\nu(\text{CO})$ region highlighted).

S2.9. Synthesis of $[\text{Zr}_6\text{O}_4(\text{OH})_4(\text{BDC})_{4.8}(\text{BDC-Im-Rh}(\text{CO})_2\text{I})_{1.1}(\text{OAc})_{0.1}]$



Dry *n*-hexane (25 cm³) was added to a sample of **1** (50 mg) and $[\text{Rh}(\text{CO})_2\text{I}]_2$ (10 mg) under CO and left stirring overnight. The solids were collected via filtration and its IR spectrum (KBr disc, Figure S16) contained $\nu(\text{CO})$ absorptions at 2075 cm⁻¹ and 2007 cm⁻¹, indicating covalent incorporation of rhodium, i.e. $[\text{Zr}_6\text{O}_4(\text{OH})_4(\text{BDC})_{4.8}(\text{BDC-Im-Rh}(\text{CO})_2\text{I})_{1.1}(\text{OAc})_{0.1}]$.

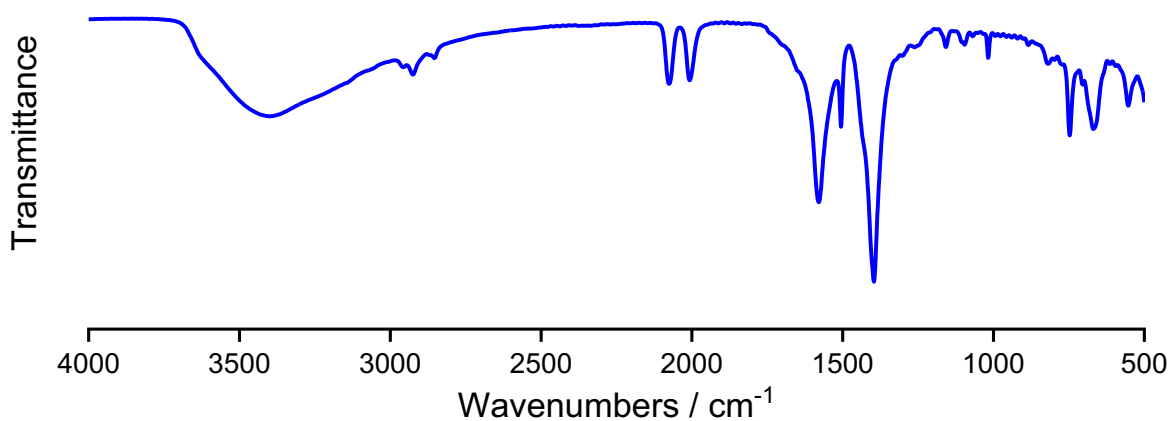


Figure S16 IR spectrum (KBr disc) of $[\text{Zr}_6\text{O}_4(\text{OH})_4(\text{BDC})_{4.8}(\text{BDC-Im-Rh}(\text{CO})_2\text{I})_{1.1}(\text{OAc})_{0.1}]$.

S2.10. Reaction of **3** with MeI and CO

A sample of **3** (10 mg) was soaked in neat MeI (5 cm³) overnight and collected by centrifugation followed by drying under high vacuum overnight. The ATR-IR spectrum of the product (Figure S17) contained a $\nu(\text{CO})$ absorption at 2060 cm⁻¹ as well as a broad band at 1735 cm⁻¹. The dry oxidative addition product was then exposed to a CO atmosphere for 10 d, and the ATR-IR spectrum of the product (Figure S17) contained $\nu(\text{CO})$ absorptions at 2088 cm⁻¹ and 1694 cm⁻¹.

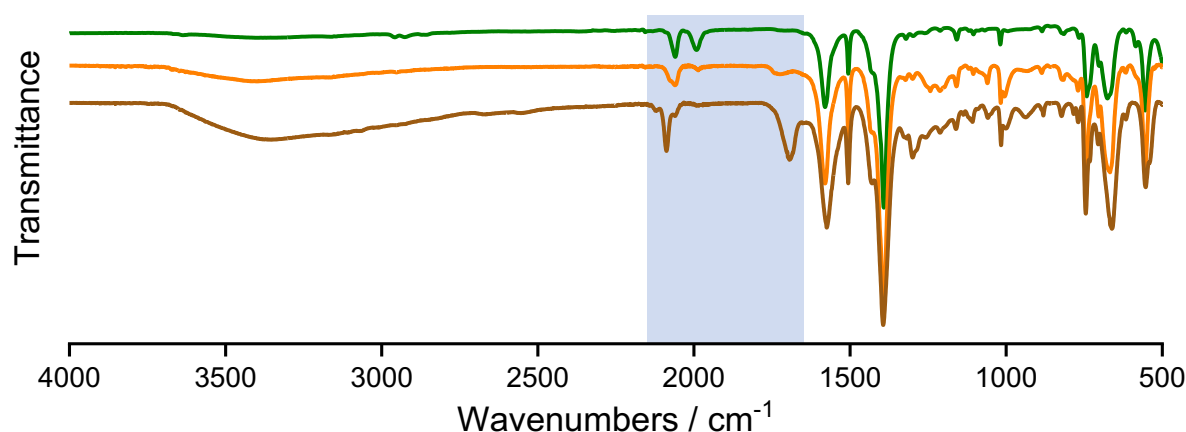


Figure S17 Infrared spectra (ATR-IR, $\nu(\text{CO})$ region highlighted) of **3** (green), after soaking in MeI overnight (orange), after exposure to CO atmosphere for 10 days (brown).

S2.11. Catalytic carbonylation of MeOH with **3**

Methanol carbonylation reactions were monitored *in situ* by high-pressure IR spectroscopy using a cylindrical internal reflectance (CIR) cell comprising an autoclave (Parr) modified to accommodate a crystalline silicon CIR rod, as described previously.⁹ Spectra were recorded using a Perkin-Elmer Spectrum GX FTIR spectrometer fitted with an MCT detector. The cell was placed directly in the spectrometer sample compartment and aligned to maximize IR energy throughput using a tilt table. A background spectrum was recorded using the appropriate solvent mixture at 120 °C.

Dry CHCl₃ (5 cm³) was added to **2** (100 mg) and [Rh(CO)₂I]₂ (10 mg, 0.017 mmol) under CO gas to generate supported catalyst **3** *in situ*. The mixture was sonicated for 30 minutes and stirred for 16 h at RT. Meanwhile, MeI (0.5 cm³) and dry MeOH (1 cm³) were added to a 5 cm³ volumetric flask which was made up to the mark with dry CHCl₃. This mixture of solvents and

the previously prepared suspension were added to the CIR cell, which was flushed 5 times with CO, then pressurised with CO (10 bar) and heated to 120 °C. Four scans were taken for each IR spectrum at 5 min intervals over the course of four hours, to monitor the appearance of an absorption due to MeOAc at 1741 cm⁻¹ (Figure S18).

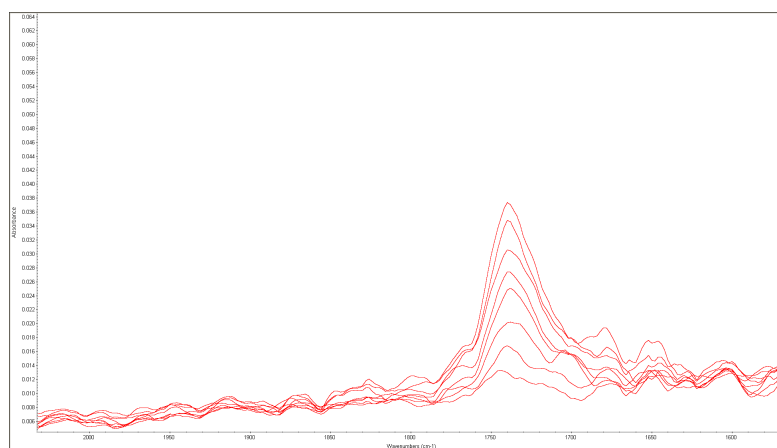


Figure S18. Series of IR spectra showing the growth of absorption at 1741 cm⁻¹ due to MeOAc during catalytic carbonylation reaction using **3** (10 bar CO, 0.8 M MeI, 2.5 M MeOH in CHCl₃ at 120 °C).

The rate of formation of methyl acetate was measured from the gradient of a plot of absorbance vs. time for the $\nu(\text{C}=\text{O})$ band of methyl acetate at 1741 cm⁻¹ (0.0045 h⁻¹). Dividing this value by the measured effective extinction coefficient for methyl acetate in CHCl₃ using the same cell (0.193 mol⁻¹ dm³) and multiplying this by the volume (0.01 dm³) gives a value for the rate of formation of methyl acetate as 2.33×10^{-4} mol h⁻¹. To calculate the turnover frequency (TOF), this value was divided by the total number of moles of rhodium in the system (3.53×10^{-5} mol) to give a TOF value of 6.60 h⁻¹.

At the end of the experiment, the solid was recovered *via* centrifugation and a powder X-ray diffraction pattern was recorded (Figure S19) and fitted using TOPAS Academic version 4.1 as an $Fm\bar{3}m$ space group where $a = 20.769(3)$ Å (Section S3). An IR spectrum of the recovered solid is shown in Figure S20.

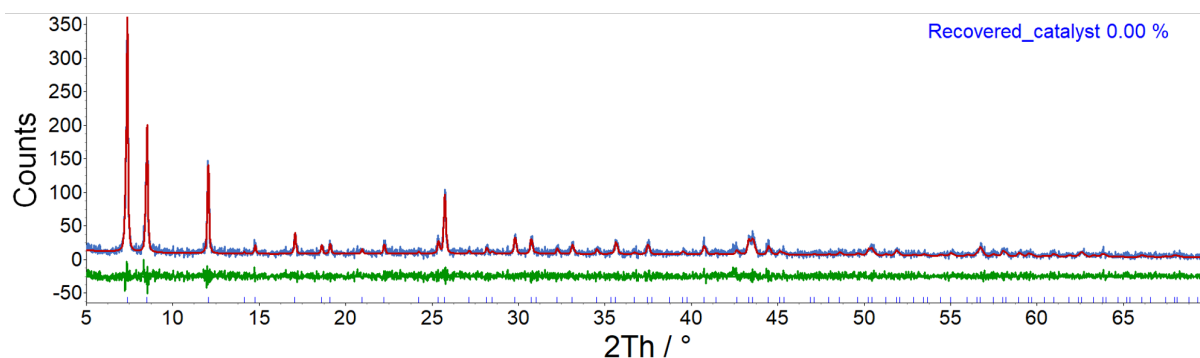


Figure S19 Pawley fit of recovered solid from catalysis experiment showing the observed pattern (blue), the fit (red), and the difference (green). $5 \leq 2\theta \leq 70^\circ$; $d_{\min} 1.34 \text{ \AA}$.

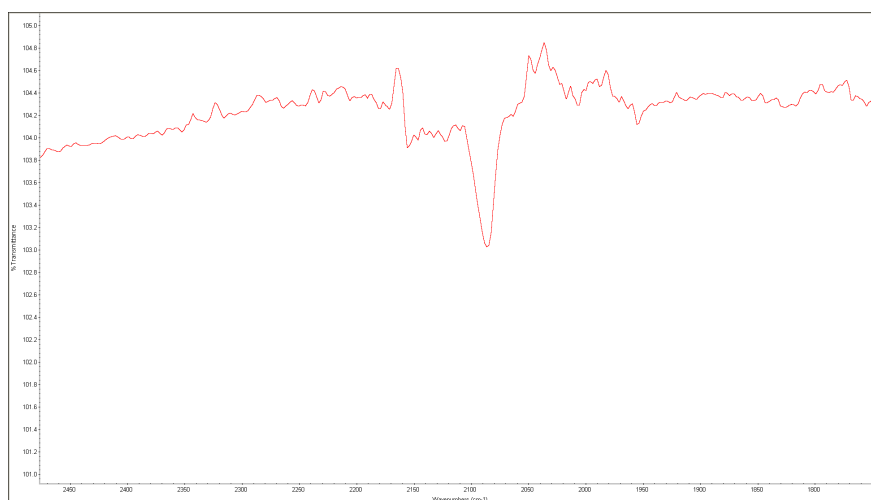


Figure S20 ATR IR spectrum of recovered solid from catalysis experiment showing $\nu(\text{CO})$ band at 2086 cm^{-1} assigned to $\text{trans-}[\text{Rh}(\text{CO})_2(\text{COMe})\text{I}_3]^-$.

To demonstrate the recyclability of the catalyst, the recovered solid was added to the cell along with dry CHCl_3 (8.5 cm^3), MeI (0.5 cm^3) and dry MeOH (1 cm^3) and a further carbonylation experiment was performed as described above to demonstrate that the catalyst had retained its activity following recycling.

For comparison an experiment was carried out under identical conditions but using $n\text{-Bu}_4\text{NI}$ (13 mg , 0.035 mmol) in place of **2** to generate homogeneous $[\text{Rh}(\text{CO})_2\text{I}_2]\text{Bu}_4\text{N}$ from $[\text{Rh}(\text{CO})_2\text{I}]_2$ *in situ*. The TOF value was calculated as described above.

S3.Pawley fitting parameters

All patterns were fitted as cubic $Fm\bar{3}m$ space groups using nine background parameters, one zero-point parameter and five peak profile parameters.

Indexing and Pawley refinements were carried out using TOPAS Academic version 4.1.⁴

Indices of fit between the calculated and experimental diffraction patterns (R_{wp} and R_{wp}') are defined by Equation S1 and Equation S2 respectively.

$$R_{wp} = \sqrt{\frac{\sum[w(Y_{obs} - Y_{calc})^2]}{\sum[wY_{obs}^2]}}$$

Equation S1

$$R_{wp}' = \sqrt{\frac{\sum[w(Y_{obs} - Y_{calc})^2]}{\sum[w(Y_{obs} - bkgr)^2]}}$$

Equation S2

Table S2 Data from Pawley phase fits of MOF materials.

Sample	$a / \text{\AA}$	R_{wp}	R_{wp}'	Reflections
$[\text{Zr}_6\text{O}_4(\text{OH})_4(\text{BDC})_6]$	20.8054(5)	8.2	10.6	131
$[\text{Zr}_6\text{O}_4(\text{OH})_4(\text{BDC-Im})_6]$	20.7881(3)	7.7	13.3	131
$[\text{Zr}_6\text{O}_4(\text{OH})_4(\text{BDC-Im})_{0.9}(\text{BDC-Im-Me})_{5.1}][\text{I}]_{5.1}$	20.813(1)	10.4	39.7	131
1	20.739(2)	8.0	13.5	131
2	20.750(1)	14.9	26.1	131
3	20.760(1)	8.3	11.5	131
Recovered solid post-catalysis	20.769(3)	32.7	58.3	131

S4. References

1. A. B. Pangborn, M. A. Giardello, R. H. Grubbs, R. K. Rosen and F. J. Timmers, *Organometallics*, 1996, **15**, 1518-1520.
2. A. Fulford, C. E. Hickey and P. M. Maitlis, *J. Organomet. Chem.*, 1990, **398**, 311-323.
3. G. S. Pawley, *J. Appl. Crystallogr.*, 1981, **14**, 357-361.
4. A. A. Coelho, *TOPAS Academic Version 4.1*, see <http://www.topas-academic.net>.
5. A. A. Coelho, *J. Appl. Crystallogr.*, 2018, **51**, 210-218.
6. A. A. Coelho, J. S. O. Evans, I. R. Evans, A. Kern and S. Parsons, *Powder Diffr.*, 2011, **26**, S22-S25.
7. J. Liang, R. P. Chen, X. Y. Wang, T. T. Liu, X. S. Wang, Y. B. Huang and R. Cao, *Chem. Sci.*, 2017, **8**, 1570-1575.
8. J. Liang, Y. Q. Xie, X. S. Wang, Q. Wang, T. T. Liu, Y. B. Huang and R. Cao, *Chem. Commun.*, 2018, **54**, 342-345.
9. W. R. Moser, J. E. Cnossen, A. W. Wang and S. A. Krouse, *J. Catal.*, 1985, **95**, 21-32.